Baseband Distortion Modeling for a Parametric Loudspeaker System Using Volterra Kernels

Wei Ji, Ee-leng Tan, Woon-Seng Gan
Digital Signal Processing Laboratory, School of Electrical and Electronic Engineering
Nanyang Technological University, Singapore
E-mail: {wji, etanel, ewsgan}@ntu.edu.sg

***Abstract*— A directional sound beam can be generated by a parametric loudspeaker system through the nonlinear interaction between finite-amplitude ultrasonic waves in air. However, this nonlinear interaction also produces harmonic components in addition to the desired audible sound. In order to investigate this nonlinear phenomenon, a baseband distortion model is developed from nonlinear system identification using Volterra kernels along with results obtained from both numerical simulations and experimental measurements that take into account the emitter's response. A nonlinear model with reduced complexity to the 2nd-order Volterra kernel is found to agree with the mathematical model. Based on this model, we can predict the total harmonic distortion (THD) in the far field and perform predistortion technique to remove it.**

I. INTRODUCTION

The original prototype of parametric loudspeaker in air was firstly studied experimentally by Bernett and Blackstock in the 1970s [1]. The nonlinear interaction between two finite-amplitude ultrasonic waves, which are referred as primary waves, can give rise to an end-fire array of virtual sources along the propagation path. Thus, a difference frequency sound beam, which retains the high directivity of the ultrasonic waves, is generated. Due to this nonlinear mechanism, an audible sound modulating an ultrasonic carrier at the input of the parametric loudspeaker system can be reproduced at the output of the system. However, the frequency band of the demodulated secondary sound is extended from the original baseband with the generation of harmonics in the self-demodulation process, which distorts the desired baseband signal and degrades the sound quality. Considerable studies have been carried out on how to mitigate the distortion brought about by the conventional double-sideband amplitude modulation (DSBAM) with improved modulation techniques, which mainly consist of single-sideband amplitude modulation (SSBAM) [2], square-root amplitude modulation (SRAM) [3], and modified amplitude modulation (MAM) [4]. The advantages and disadvantages of these modulation techniques have been studied theoretically and experimentally in [5] with a conventional piezoelectric ultrasonic emitter array.

The Volterra filter is widely used in modeling the nonlinear mechanism of a nonlinear system, rendering the system input-output equation as a polynomial series. For example, the nonlinear process in horns and ducts has been studied by Klippel using a Volterra series expansion up to the *n*th-order kernels [6]. The *n*th-order Volterra filter has the advantage of modeling the nonlinear system with a straightforward filter structure, which is capable of approximating the nonlinear system with finite number of coefficients [7]. With reference to the previous theoretical study of parametric loudspeaker systems, the distortion is largely attributed to the second harmonic in the demodulated signal, especially when the DSBAM technique is used [8]. Therefore, in this paper, a baseband distortion model is developed using an adaptive Volterra filter consisting of the 1st- and 2nd-order kernels, which is able to predict the sound pressure levels (SPL) of the reproduced baseband term (fundamental) and the nonlinear quadratic term (second harmonic) in the sound field.

The rest of this paper is organized as follows. Section 2 gives a brief overview of the parametric loudspeaker system. Section 3 describes the adaptive structure and algorithms for computing the coefficients of the 1st- and 2nd-order Volterra kernels. In Section 4, numerical simulations of the Volterra kernels are conducted to match the theoretical output of the parametric loudspeaker system based on a mathematical model. Measurements are carried out to train the adaptive filter for modeling the actual system, and the modeling performance is evaluated in Section 5. Finally, Section 6 concludes this paper.

II. PARAMETRIC LOUDSPEAKER SYSTEM

The acoustic parametric effect occurs when the parametric loudspeaker system operates in the nonlinear region of finite-amplitude ultrasounds propagation in air. The consequence of this nonlinear phenomenon is the generation of an audible sound beam retaining the high directivity of the ultrasounds.

Instead of transmitting multiple ultrasonic frequencies to generate audible signals in air, the parametric loudspeaker system is able to reproduce the desired audible sound by modulating an ultrasonic carrier using various modulation techniques at the system input stage. As shown in Fig. 1, the input baseband audible sound modulates the ultrasonic carrier to form a modulated signal, which is channeled by a power amplifier to drive the ultrasonic emitter to operate at a suitable pressure level for achieving the acoustic parametric effect in air. Due to the nonlinear interaction between the primary waves, the desired signal is reproduced from the end-fire virtual source array but suffers from harmonic distortion. Generally, the system output end is referred as a certain listening zone away from the ultrasonic emitter. In this paper,

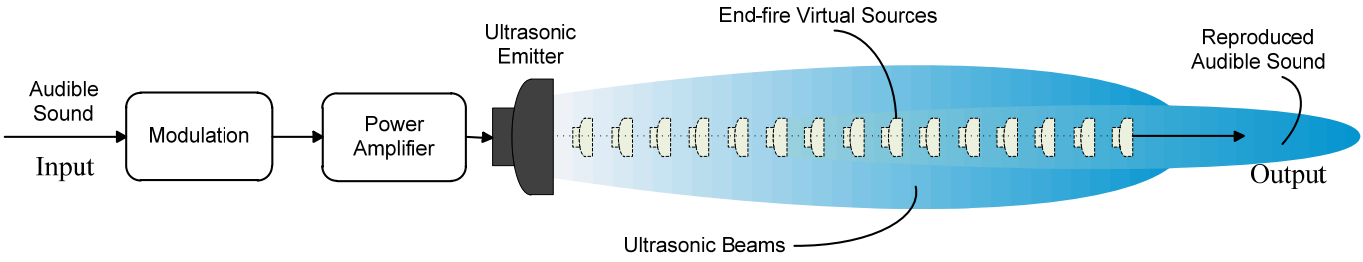

Fig. 1 Block diagram of a parametric loudspeaker system.

the nonlinear distortion present in the reproduced baseband signal is examined using the DSBAM scheme and the output end is observed at the Rayleigh distance on the propagation axis.

III. Adaptive Volterra Filter

The polynomial-series-based Volterra filter is very popular in modeling a causal and time-invariant nonlinear system with the following series expansion [9]

$$y(n) = h_0 + \sum_{i=1}^{\infty}\sum_{m_1=0}^{\infty}\sum_{m_2=0}^{\infty}\cdots\sum_{m_i=0}^{\infty}\left[h_i(m_1,m_2,\cdots,m_i)\cdot\prod_{j=1}^{i}x(n-m_j)\right], \tag{1}$$

where $x(n)$ and $y(n)$ represent the input and output signals, respectively. $h_i(m_1,m_2,\cdots,m_p)$ is defined as the ith-order Volterra kernel, and h_0 can generally be ignored [9]. In this paper, we focus on using the Volterra filter to model the linear and quadratic nonlinear output of the parametric loudspeaker system. Thus, a truncated Volterra series expansion up to the 2nd-order kernel is utilized and can be expressed as

$$\begin{aligned} y(n) &= \sum_{m_1=0}^{N_1-1} h_1(m_1)x(n-m_1) \\ &\quad + \sum_{m_2=0}^{N_2-1}\sum_{m_1=0}^{N_2-1} h_2(m_1,m_2)x(n-m_1)x(n-m_2), \end{aligned} \tag{2}$$

where N_1 and N_2 are the memory lengths of the kernels $\mathbf{H}_1[\cdot]$ and $\mathbf{H}_2[\cdot]$, respectively. The Volterra system identification process is implemented by using a cascaded adaptive structure combining the 1st- and 2nd-order kernels, as illustrated in Fig. 2.

In Fig.2, the parametric loudspeaker system takes the input signal $x(n)$ as the modulating signal. Through the nonlinear interaction occurring between the primary waves projected by the ultrasonic emitter, the self-demodulated secondary sound $d(n)$ is generated, consisting of the reproduced baseband signal and higher-order harmonics. Adaptations for the 1st- and 2nd-order kernels are carried out simultaneously during the identification process. The 1st-order kernel serves to model the linear component in $d(n)$ with error $e_1(n)$ feeding back to adapt the 1st-order kernel. In addition, the residual signal $e_1(n)$ is also sent to the 2nd-order kernel in the second-

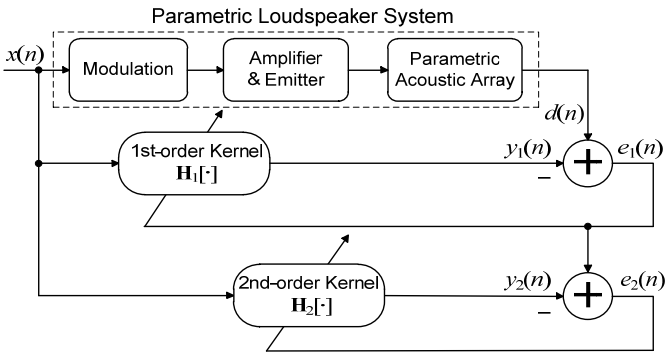

Fig. 2 Block diagram of the adaptive Volterra structure.

stage adaptation, in which the coefficients $h_2(m_1,m_2)$ are used to model the quadratic component present in $e_1(n)$ by feeding back error signal $e_2(n)$ to update $\mathbf{H}_2[\cdot]$.

In our proposed structure, the normalized least-mean-square (NLMS) algorithm is employed as the adaptive algorithm, which is based on the steepest decent approach to minimize the squared error signal at each iteration. With the cascaded adaptive structure, the coefficients of the 1st- and 2nd-order kernels are adapted using the NLMS algorithm as follows

$$h_1(m_1;n+1) = h_1(m_1;n) + \mu_1(n)e_1(n)x(n-m_1), \tag{3}$$

$$h_2(m_1,m_2;n+1) = h_2(m_1,m_2;n) + \mu_2(n)e_2(n)x(n-m_1)x(n-m_2), \tag{4}$$

where the time-varying step size $\mu_1(n)$ and $\mu_2(n)$ are given as

$$\mu_1(n) = \frac{\mu_0}{\mathbf{X}_1^T(n)\mathbf{X}_1(n)}, \tag{5}$$

and

$$\mu_2(n) = \frac{\mu_0}{\mathbf{X}_2^T(n)\mathbf{X}_2(n)}. \tag{6}$$

μ_0 is the auxiliary step size, being in the range of $0<\mu_0<2$. The input vector $\mathbf{X}_1(n)$ and $\mathbf{X}_2(n)$ for the 1st- and 2nd-order kernels are given as

$$\mathbf{X}_1(n) = [x(n)\ \cdots\ x(n-i)\ \cdots\ x(n-N_1+1)]^T, \tag{7}$$

and

$$\mathbf{X}_2(n) = [x^2(n)\ \cdots\ x(n-j)x(n-k)\ \cdots\ x^2(n-N_2+1)]^T. \tag{8}$$

IV. Numerical Simulation

It is well known that the Khokhlov-Zabolotskaya-Kuznetsov (KZK) nonlinear parabolic wave equation [10], which accounts for the combined effects of diffraction, absorption and nonlinearity, is capable of giving an accurate description of the propagation characteristics of finite-amplitude sound beams. For axisymmetric sound beams propagating in the z direction, the KZK equation can be written as

$$\frac{\partial^2 p}{\partial z \partial \tau} = \frac{c_0}{2}\left(\frac{\partial^2 p}{\partial r^2} + \frac{1}{r}\frac{\partial p}{\partial r}\right) + \frac{D}{2c_0^3}\frac{\partial^3 p}{\partial \tau^3} + \frac{\beta}{2\rho_0 c_0^3}\frac{\partial^2 p^2}{\partial \tau^2}, \qquad (9)$$

where p is the sound pressure, $\tau = t - z/c_0$ is the retarded time, r is the radial distance from z axis, c_0 is the small signal sound speed, ρ_0 is the ambient density of the medium, D is the sound diffusivity, and β is the nonlinear coefficient. As there is no explicit analytic solution of the KZK equation, a numerical solution in time domain is developed by Lee *et al.* [11] on the basis of a transformed expression of (10) as

$$\frac{\partial P}{\partial \sigma} = \frac{1}{4(1+\sigma)^2}\int_{-\infty}^{\tau}\left(\frac{\partial^2 P}{\partial \rho^2} + \frac{1}{\rho}\frac{\partial P}{\partial \rho}\right)d\tau' + A\frac{\partial^2 P}{\partial \tau^2} + \frac{NP}{1+\sigma}\frac{\partial P}{\partial \tau}. \qquad (10)$$

For simplicity, we only focus on two important parameters A and N, the detailed derivation can be referred to [11]. $A = \alpha_0 z_0$ is the absorption parameter and $N = z_0/\bar{z}$ is the nonlinearity parameter, where α_0 is the attenuation coefficient, z_0 is the Rayleigh distance, and $\bar{z}$ represents the plane wave shock formation distance.

Based on the numerical solution of (10), simulation is conducted to model the linear and quadratic nonlinear output of the parametric loudspeaker system, where a band-limited white noise signal is presented as the system input $x(n)$. The frequency of the white noise input ranges from 0 to 5 kHz and the amplitude is uniformly distributed between −1 to 1. A 40 kHz ultrasonic carrier is modulated by the input with modulation index $m = 0.8$ to form the DSBAM primary waves. The desired signal $d(n)$ is computed numerically from the KZK equation for the adaptation process shown in Fig. 2, in which the memory length of the 1st- and 2nd-order kernels is 100 and the auxiliary step size μ_0 is 0.5. It is observed in Fig. 3 that the mean-square error (MSE) values for $e_1(n)$ and $e_2(n)$ after 3.2×10^4 iterations reduce steadily down to around −13 dB and −18 dB, respectively.

The steady-state coefficients of the 2nd-order kernel are plotted in Fig. 4. We notice that the dominant coefficient for the 2nd-order kernel is located at $h_2(0,0)$ while the other coefficients are insignificant. This observation implies that the quadratic nonlinear effect in the parametric loudspeaker system is largely memoryless and can be approximated by using a square function.

V. Experimental Measurement

In this section, the parametric loudspeaker system is modeled with the previous Volterra filter by using the desired signal from experimental measurements that take into account the emitter's frequency response, and the Volterra modeling performance is evaluated based on SPL and THD obtained from the experiments.

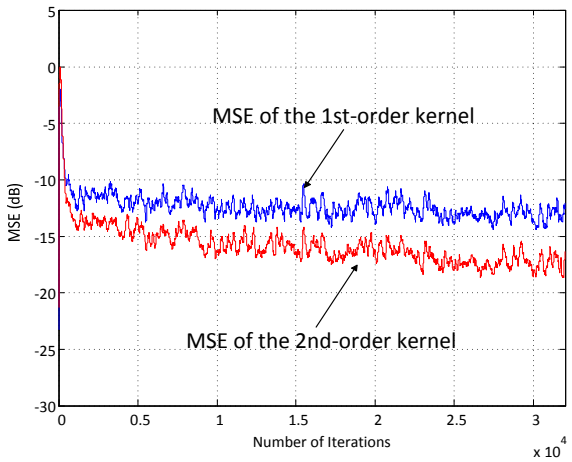

Fig. 3 MSE of the 1st- and 2nd-order Volterra kernels from numerical simulations.

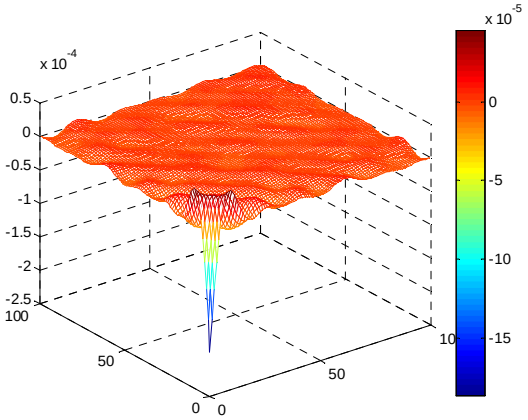

Fig. 4 Final coefficients of the 2nd-order kernel from numerical simulations.

A. Nonlinear Modeling

Experiments were carried out for the actual secondary sound in an anechoic chamber with dimensions of 6 m long, 4 m wide, and 3.5 m high. Fig. 5 shows the block diagram of the experimental setup: A floating-point DSP platform implements the DSBAM signal and sends the modulated signal to a class-D power amplifier with low phase shift and output noise. An ultrasonic emitter consisting of 253 piezoelectric transducer units, which resonates at 40 kHz, is driven at a suitable voltage level to achieve the parametric effect in air. The demodulated secondary sound is captured by a B&K Type 4134 1/2-inch microphone attached to a Type 3110 module for a duration of 5 seconds per time capture at an axial distance of 4 m away from the emitter source. The captured signal is low-pass filtered at 20 kHz cut-off frequency to remove any ultrasonic signal, before computing errors for the adaptive Volterra cascade structure.

In the experimental measurement, an input white noise signal with the same characteristics as the one discussed in Section IV is fed to the parametric loudspeaker system to train

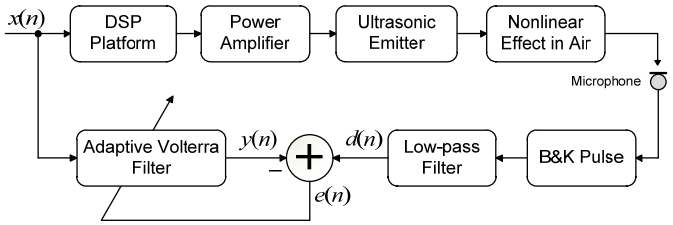

Fig. 5 Block diagram of experimental setup.

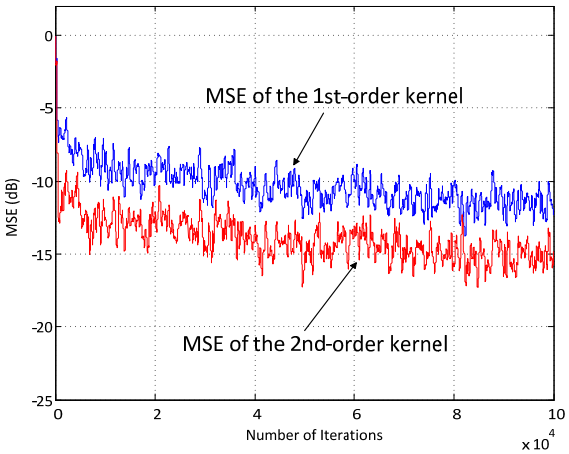

Fig. 6 MSE of the 1st- and 2nd-order Volterra kernels from measurements.

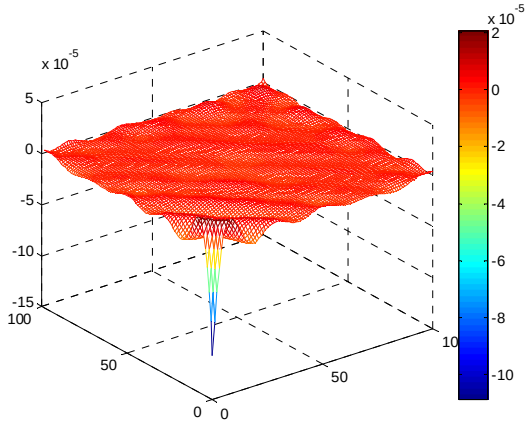

Fig. 7 Final coefficients of the 2nd-order kernel from measurements.

the adaptive Volterra filter for modeling the nonlinear system. With the adaptive structure shown in Fig. 2 and the same adaptive parameters for the 1st- and 2nd-order kernels as those in the simulations, the nonlinear model is trained for 1×10^5 iterations. In Fig. 6, we can see that the MSE values for $e_1(n)$ and $e_2(n)$ stabilize approximately at -12 dB and -15 dB, respectively. Fig. 7 shows the final coefficients of the 2nd-order kernel using $d(n)$ from the measurements that accounts for the emitter's frequency response. It is noted that the trend of coefficients of the 2nd-order kernel agrees well with that obtained in the simulations, which indicates that the quadratic nonlinearity largely depends on $h_2(0,0)$ and the frequency response of the ultrasonic emitter does not affect the location of the dominant coefficient in the nonlinear modeling.

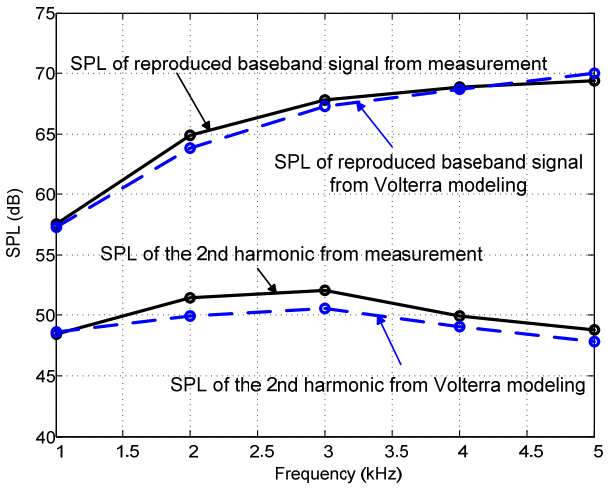

Fig. 8 SPL of the reproduced baseband signal and the 2nd harmonic obtained from measurements and Volterra model.

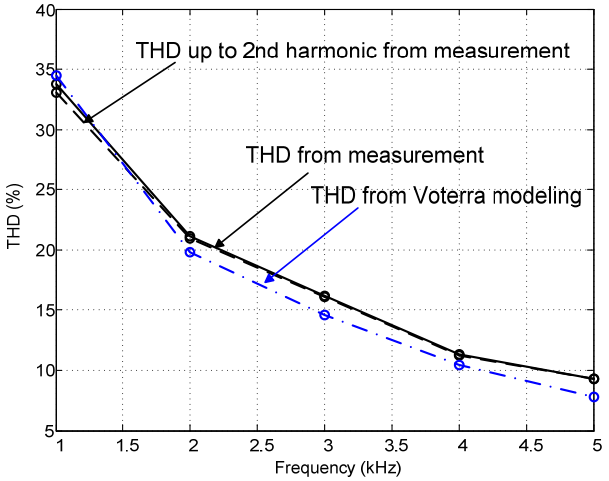

Fig. 9 THD levels obtained from measurements and Volterra model.

B. *Modeling Performance*

In this subsection, the performance of the nonlinear system modeling is examined by passing five single tones from 1 kHz to 5 kHz through the parametric loudspeaker system and the Volterra filter with the steady-state coefficients obtained from the previous subsection. SPL and THD are calculated and compared between the Volterra filter output using the final coefficients from the model training and the secondary sound from the measurements, respectively.

Fig. 8 shows the SPL of the reproduced baseband signal and the second harmonic from the measurements and the Volterra modeling, respectively. It is seen that the system model outputs can closely match the measurement results with an error of less than 1 dB. . It should be noted that the narrow bandwidth of the ultrasonic emitter partially equalizes the frequency response in Fig. 8, which is flatter than the 12 dB/octave slope predicted by the mathematical model [8].

In this paper, THD is used to measure the total amount of distortion existing in the secondary sound, which is given as

$$\mathrm{THD} = \sqrt{\frac{T_2^2 + T_3^2 + \cdots + T_n^2}{T_1^2 + T_2^2 + T_3^2 + \cdots + T_n^2}} \times 100\%, \qquad (11)$$

where T_i represents the amplitude of the *i*-th harmonic in the secondary sound. The THD level can be approximated by measuring up to the 2nd harmonic as

$$\mathrm{THD}_{\mathrm{approx}} = \sqrt{\frac{T_2^2}{T_1^2 + T_2^2}} \times 100\%. \qquad (12)$$

Fig. 9 shows the THD calculated from the measurements based on (11) and (12), as well as from the Volterra modeling up to 2nd-order kernel. It is found that the measured THD level calculated from (2) is almost identical to that from (1), which verifies that the baseband distortion is largely attributed to the contribution of the second harmonic. In addition, the THD predicted by the Volterra modeling can match the measured THD with only small errors.

VI. Conclusions

In this paper, we developed a baseband distortion model based on the 1st- and 2nd-order Volterra kernels for studying the nonlinear effect in the demodulated secondary sound of a parametric loudspeaker system. The well-known NLMS algorithm was used in the nonlinear system identification with a cascaded adaptive Volterra filter structure. It has been found that the Volterra kernels are suitable in modeling the nonlinear distortion present in the reproduced baseband signal from the numerical simulations and experimental measurements. The comparison between the two sets of kernel coefficients derived from the theoretical equation and experimental measurements shows good agreement and indicates that the quadratic nonlinear term is largely memoryless and can be approximated by a square function. The effectiveness of using the Volterra model has also been verified by the good agreement between modeling prediction and measurement results in terms of SPL and THD. Therefore, predistortion techniques based on the Volterra model can be more efficiently implemented to reduce the overall distortion in parametric loudspeaker systems.

References

[1] M. B. Bennett and D. T. Blackstock, "Parametric array in air," *J. Acoust. Soc. Am*, vol. 57, pp. 562-568, March 1975.

[2] T. Kamakura, Y. Tasahide, and K. Ikeyaya, "A study for the realization of a parametric loudspeaker," *J. Acoust. Soc. Jpn*, pp. 1-18, June 1985.

[3] T. D. Kite, J. T. Post, and M. F. Hamilton, "Parametric array in air: Distortion reduction by preprocessing," in *Proc. 16th Int. Cong. Acoust.*, vol.2, pp. 1091-1092, 1998.

[4] E. L. Tan, W. S. Gan, P. F. Ji, and J. Yang, "Distortion analysis and reduction for the parametric array," in *Proc. 124th Conv. Audio Eng. Soc.*, 2008.

[5] W. Ji, P. F. Ji, and W. S. Gan, "Theoretical and experimental comparison of amplitude modulation techniques for parametric loudspeakers," in *Proc. 128th Conv. Audio Eng. Soc.*, 2010.

[6] W. Klippel, "Nonlinear wave propagation in horns and ducts," *J. Acoust. Soc. Am*, vol. 98, pp. 431-436, July 1995.

[7] V. J. Mathews and G. L. Sicuranza, *Polynomial Signal Processing*, New York: Wiley and Sons, 2000.

[8] M. Yoneyama and J. Fujimoto, "The audio spotlight: An application of non-linear interaction of sound waves to a new type of loudspeaker design," *J. Acoust. Soc. Am*, vol. 73, pp. 1532-1536, May 1983.

[9] V. J. Mathews, "Adaptive polynomial filters," *IEEE Sig. Proc. Mag.*, vol. 8, pp. 10-26, July 1991.

[10] M. F. Hamilton and D. T. Blackstock, Nonlinear Acoustics, San Diego, CA: Academic, 1998

[11] Y. S. Lee, "Numerical solution to the KZK equation for pulsed finite amplitude sound beams in thermoviscous fluids," PhD. Dissertation, University of Texas at Austin, 1993.